NASA TECHNICAL NOTE

NASA TN D-3702

NASA TN D-3702

# BENDING TESTS OF TWO LARGE-DIAMETER CORRUGATED CYLINDERS WITH ECCENTRIC RING STIFFENERS

*by James Kent Anderson*

*Langley Research Center*

*Langley Station, Hampton, Va.*

NATIONAL AERONAUTICS AND SPACE ADMINISTRATION • WASHINGTON, D. C. • NOVEMBER 1966

*The information presented herein is based in part upon a thesis offered in partial

# BENDING TESTS OF TWO LARGE-DIAMETER CORRUGATED CYLINDERS WITH ECCENTRIC RING STIFFENERS*

By James Kent Anderson
Langley Research Center

## SUMMARY

Results of bending tests on two large-diameter aluminum-alloy corrugated cylinders with eccentric (one-sided) stiffening rings are presented. The cylinders were identical except for the location of stiffening rings; one cylinder had rings attached to the external surface of the cylinder, the other had rings attached to the internal surface. Both cylinders buckled in a general-instability mode involving buckling of the corrugated wall and reinforcing rings as a composite wall. The buckling strength of the cylinder with rings attached to the external surface was 2.3 times that of the cylinder with rings attached to the internal surface. Both cylinders buckled at approximately 70 percent of the load predicted by the use of a small-deflection buckling theory which included the effect of stiffening ring eccentricity.

## INTRODUCTION

The ring-stiffened corrugated cylinder is an attractive low-mass—high-strength structure for interstage and intertank sections of launch vehicles. Five buckling tests are reported in reference 1 which supply design data for such structures. In these tests, the stiffening rings were attached to the inside surface of the corrugated walls of the test cylinders. These cylinders buckled in the general instability mode (mode entailing buckling of the corrugated wall and rings as a composite wall) at loads that were approximately 75 percent of the buckling loads predicted by the use of a small-deflection buckling theory (ref. 2). This theory predicts a large influence on buckling from ring eccentricity.

The present investigation was undertaken to investigate the role played by ring eccentricity in the discrepancy between theoretical predictions and test results. In this investigation, tests similar to those of reference 1 were conducted on two cylinders which differed only in ring location. One cylinder had rings attached to the inside surface of the cylinder wall whereas the other had identical rings attached to the outside surface. These

---

*The information presented herein is based in part upon a thesis offered in partial fulfillment of the requirements for the degree of Master of Science in Engineering Mechanics, Virginia Polytechnic Institute, Blacksburg, Virginia, June 1966.

test cylinders were similar to those of reference 1 but differed in some details so that general instability buckling would occur in both cylinders.

A supplementary test was made in reference 1 to determine the effect of the type of attachment between the stiffening rings and corrugated wall on the cylinder buckling strength. A similar test was made in the present investigation to substantiate the conclusion of reference 1 that the addition of stiffening clips to the attachment junction between the corrugated wall and stiffening rings was ineffectual in changing the buckling load of the cylinders. The present test is discussed in appendix A.

## SYMBOLS

The units used for physical quantities defined in this paper are given both in the U.S. Customary Units and in the International System of Units (SI) (ref. 3). Factors relating the two systems are given in appendix B.

| | |
|---|---|
| $E$ | Young's modulus of cylinder material |
| $l$ | ring spacing |
| $M$ | bending moment applied to test cylinder |
| $m$ | number of half-waves in cylinder buckle pattern in axial direction |
| $n$ | number of full-waves in cylinder buckle pattern in circumferential direction of cylinder loaded in uniform axial compression |
| $N_x$ | load per unit length of cylinder circumference at buckling and failure |
| $R$ | radius of cylinder measured to centroid of corrugated wall |
| $t$ | sheet thickness of corrugated wall of cylinder |

Subscripts:

| | |
|---|---|
| cr | critical |
| ult | ultimate |

## TEST SPECIMENS AND TEST PROCEDURE

The test specimens consisted of two circular cylinders with corrugated walls; each cylinder had eleven equally spaced, small, closed, hat-section rings. The two cylinders differed from each other only in location of stiffening rings. One cylinder had the stiffening rings attached to the outside surface of the corrugated wall (cylinder 1) and the other had rings attached to the inside surface (cylinder 2).

The photographs of figures 1 and 2 illustrate general features of the test cylinders and ring-attachment details. Other construction details are shown in figure 3 and table I. Each cylinder was fabricated from seven corrugated sheets of 7075-T6 aluminum alloy. The sheets were fastened together with two longitudinal rows of spot welds. Each stiffening ring was composed of three segments joined together by doublers welded to the rings at each joint. The rings were attached to the corrugated wall by rivets. Wall splices and ring joints were placed as far as possible from that portion of the cylinder to be subjected to maximum compressive stress (top of cylinder in fig. 3).

The test section of the cylinder was bounded by two large, open, hat-section rings which were 80 inches (203 cm) apart and were riveted to the inside of the cylinder wall (fig. 3). The small, hat-section, stiffening rings were equally spaced in this length. The corrugated wall outside the test section was doubled in thickness to restrict failure to the test section. The double thickness was obtained by bonding and riveting another corrugated sheet to the corrugated wall.

After each cylinder had been tested, the cylinder was removed from the test fixture and cut in half around the circumference. Thirty-five micrometer measurements were then taken around the circumference to obtain the corrugation sheet thickness. The values of thickness given in table I represent the average of these measurements. Measurements of stiffening-ring and corrugation geometry were also made. Values for these dimensions were in close agreement with the values given in figure 3.

Typical material properties were used in reducing test data. Young's modulus was taken to be $10.5 \times 10^3$ ksi (72.4 $GN/m^2$) and Poisson's ratio was taken to be 0.32.

The setup for the cylinder tests is illustrated in figure 4. The apparatus and test procedures were generally the same as those employed in the investigation of reference 1. Strain-gage instrumentation was changed somewhat from that of reference 1 in order to obtain a better determination of the stress distribution in the test cylinders under load.

## TEST RESULTS AND DISCUSSION

Selected strain-gage data from gages mounted on the test cylinders are given in figures 5 and 6. The data for wall strains were obtained from "back-to-back" gages near the extreme compression fiber of the cylinders as shown in the diagrams near the top of the figure. The data generally indicate that little wall bending was experienced by the cylinders until loads near ultimate load were reached. The horizontal dashed lines of figures 5 and 6 denote the loads at buckling. These loads were determined by the "strain-reversal" method.

The measured strain distribution in the test cylinders is compared with the calculated distribution in figures 7 and 8. The measured strain, which is shown for three longitudinal stations on the test cylinders, was obtained by averaging strains from adjacent corrugation crests and troughs. Hence, the strains represent "middle-surface" strains. The calculated strain distribution was computed with the use of the standard beam equation. The measured strains are in generally good agreement with calculated strains.

The bending moments at which the cylinders buckled and failed (reached ultimate moment) are given in table I. Both cylinders failed by buckling into a general instability mode. Cylinder 1 failed catastrophically without visible evidence of impending failure. Failure was accompanied by tearing of the corrugated wall and crimping of the reinforcing rings. (See figs. 9 and 10.) Failure of cylinder 2 was less dramatic; it was characterized by the development of a deep buckle and an accompanying loss in resistance to applied load (fig. 11). The tested cylinder appeared undamaged when viewed from the outside after load had been removed; however, the rings were crimped and torn in the vicinity of the buckle.

The test results from table I are given in figure 12 for comparison with predictions based on the small-deflection buckling theory of references 2 and 4. The uniform axial compression curves are given in figure 12 because cylinders loaded in bending often have been analyzed with uniform axial compression theories. The curves of figure 12 were computed with the use of a high-speed digital computer and with orthotropic constants defined as in reference 1. Buckling of the test cylinders occurred at loads of approximately 70 percent of the predicted buckling loads for cylinders in bending. The cylinder with outside stiffening buckled at a load 2.3 times the buckling load for the cylinder with inside stiffening. The ratio of theoretical buckling loads for the test cylinders with outside and inside stiffening is also 2.3. This result suggests that eccentricity is adequately accounted for in the calculations and that the source of the 30-percent discrepancy between theory and test must have some other basis. Possible sources of the discrepancy are discussed in reference 1 where it is concluded that the discrepancy is probably a result of shortcomings of the theory in accounting for such things as discrete rings, boundary conditions at the ends of the cylinders, initial imperfections, and prebuckling deformations. The effects of these items are discussed in detail in reference 1.

## CONCLUDING REMARKS

Results are presented on the bending tests of two large-diameter corrugated cylinders which buckled in the general instability mode. One cylinder had stiffening rings on the outside surface of the corrugated wall; the other had rings on the inside. Both cylinders buckled at approximately 70 percent of the loads calculated by theory. The cylinders were analyzed with the use of a small-deflection buckling theory for bending which takes into account the eccentricity (one-sidedness) of reinforcing members. The cylinder with outside stiffening buckled at a load 2.3 times the buckling load of the cylinder with inside stiffening. The ratio of the predicted buckling loads for the test cylinder with outside stiffening to that of the cylinder with inside stiffening was also 2.3, which suggests that ring eccentricity is adequately taken into account by the theory.

Langley Research Center,
National Aeronautics and Space Administration,
Langley Station, Hampton, Va., August 3, 1966,
124-11-06-04-23.

## APPENDIX A

## AUXILIARY TEST

One auxiliary test was conducted in the present study to complement a similar test made in the study of reference 1. In the test of reference 1, a cylinder was re-tested after adding stiffening clips between the stiffening rings and the corrugated wall and after rotating the cylinder 180° in the test fixture. The design of the clips was such that they were expected to increase the bending and axial stiffness of the ring somewhat and to restrict considerably possible deformations between the outer corrugation crests and the reinforcing rings. The cylinder failed at essentially the same load in the auxiliary test as it had failed in the original test which suggested that the clips were ineffectual in changing the buckling load. However, another possible explanation for the result is that the resistance of the cylinder to buckling was not only increased by the attachment of the stiffening clips but was also decreased by the same amount by damage to the cylinder incurred in the original test. The present test was made to investigate this possibility. The test consisted of re-testing cylinder 2 after it had been rotated 180° but without adding clips between the stiffening rings and the corrugated wall. Again the cylinder failed in the auxiliary test at essentially the same load at which it had previously failed in the original test. Therefore the resistance to buckling of the cylinder after being rotated 180° for the auxiliary test was not reduced by the original test. Because the buckling behavior of the cylinder of reference 1 and cylinder 2 of the present investigation was similar, it seems clear that the addition of the stiffening clips to the cylinder of reference 1 contributed little toward increasing the buckling load of the cylinder.

## APPENDIX B

## CONVERSION OF U.S. CUSTOMARY UNITS TO SI UNITS

The International System of Units (SI) was adopted by the Eleventh General Conference on Weights and Measures, Paris, October 1960, in Resolution No. 12 (ref. 3). Conversion factors for the units used in this report are given in the following table:

| Physical quantity | U.S. Customary Unit | Conversion factor (*) | SI Unit |
|---|---|---|---|
| Length . . . . . . . . | in. | 0.0254 | meters (m) |
| Stress, modulus . . . | ksi | $6.895 \times 10^6$ | newton/meter$^2$ (N/m$^2$) |
| Moment . . . . . . . | in-kips | 113.0 | meter-newtons (m-N) |

*Multiply value given in U.S. Customary Unit by conversion factor to obtain value in SI Unit.

Prefixes to indicate multiple of units are as follows:

| Prefix | Multiple |
|---|---|
| giga (G) | $10^9$ |
| kilo (k) | $10^3$ |
| centi (c) | $10^{-2}$ |
| milli (m) | $10^{-3}$ |

## REFERENCES


1. Peterson, James P.; and Anderson, James Kent: Bending Tests of Large-Diameter Ring-Stiffened Corrugated Cylinders. NASA TN D-3336, 1966.
2. Block, David L.: Buckling of Eccentrically Stiffened Orthotropic Cylinders Under Pure Bending. NASA TN D-3351, 1966.
3. Mechtly, E. A.: The International System of Units – Physical Constants and Conversion Factors. NASA SP-7012, 1964.
4. Block, David L.; Card, Michael F.; and Mikulas, Martin M., Jr.: Buckling of Eccentrically Stiffened Orthotropic Cylinders. NASA TN D-2960, 1965.

TABLE I

MEASURED SKIN THICKNESSES AND TEST RESULTS

| Cylinder | Stiffener location | t | | $M_{cr}$ | | $M_{ult}$ | |
|---|---|---|---|---|---|---|---|
| | | inches | mm | inch-kips | km-N | inch-kips | km-N |
| 1 | External | 0.0205 | 0.521 | 4740 | 536 | 4780 | 540 |
| 2 | Internal | .0206 | .523 | 2080 | 235 | 2260 | 255 |

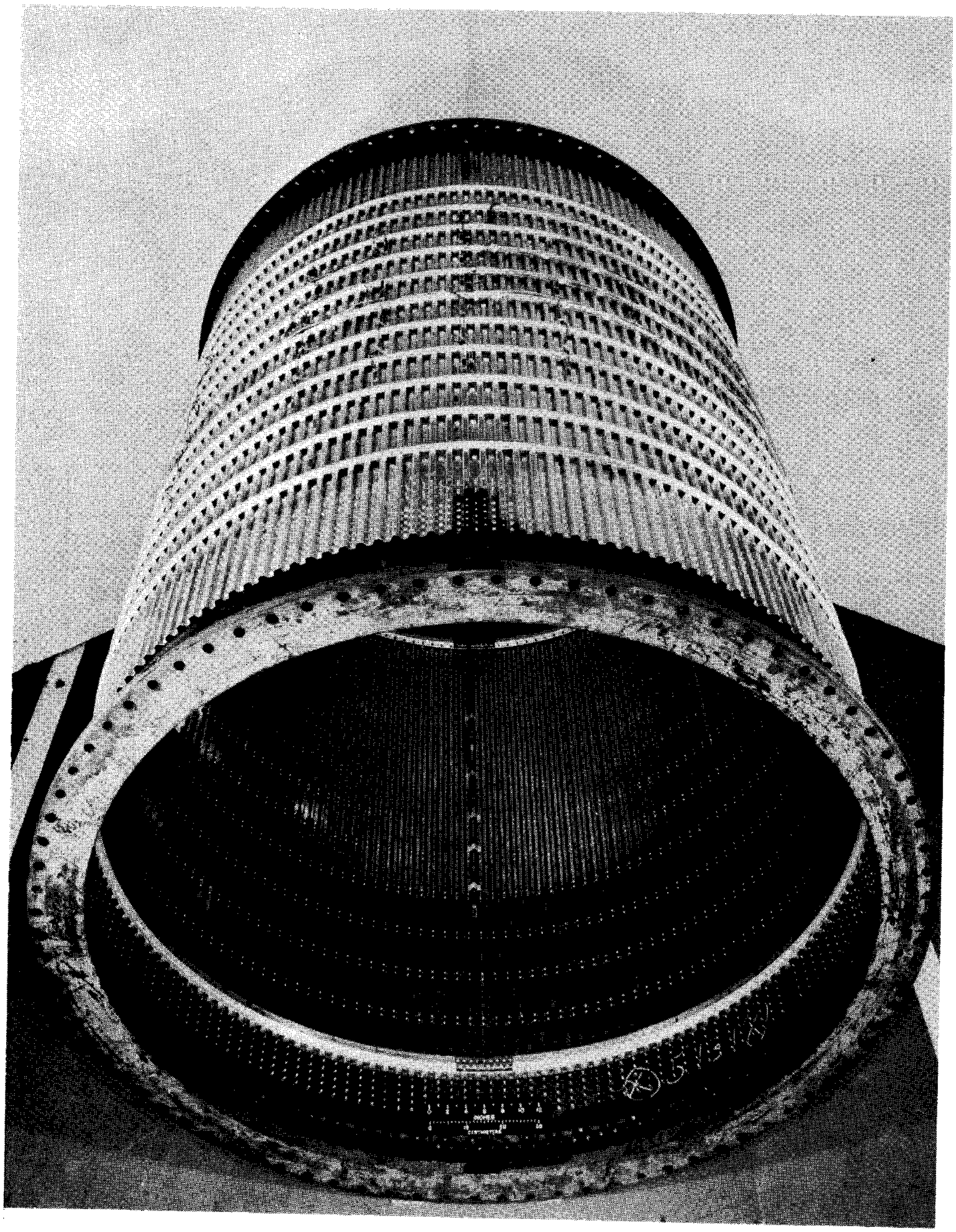

(a) General view.

L-65-6169

Figure 1.- Cylinder 1. Externally stiffened corrugated cylinder.

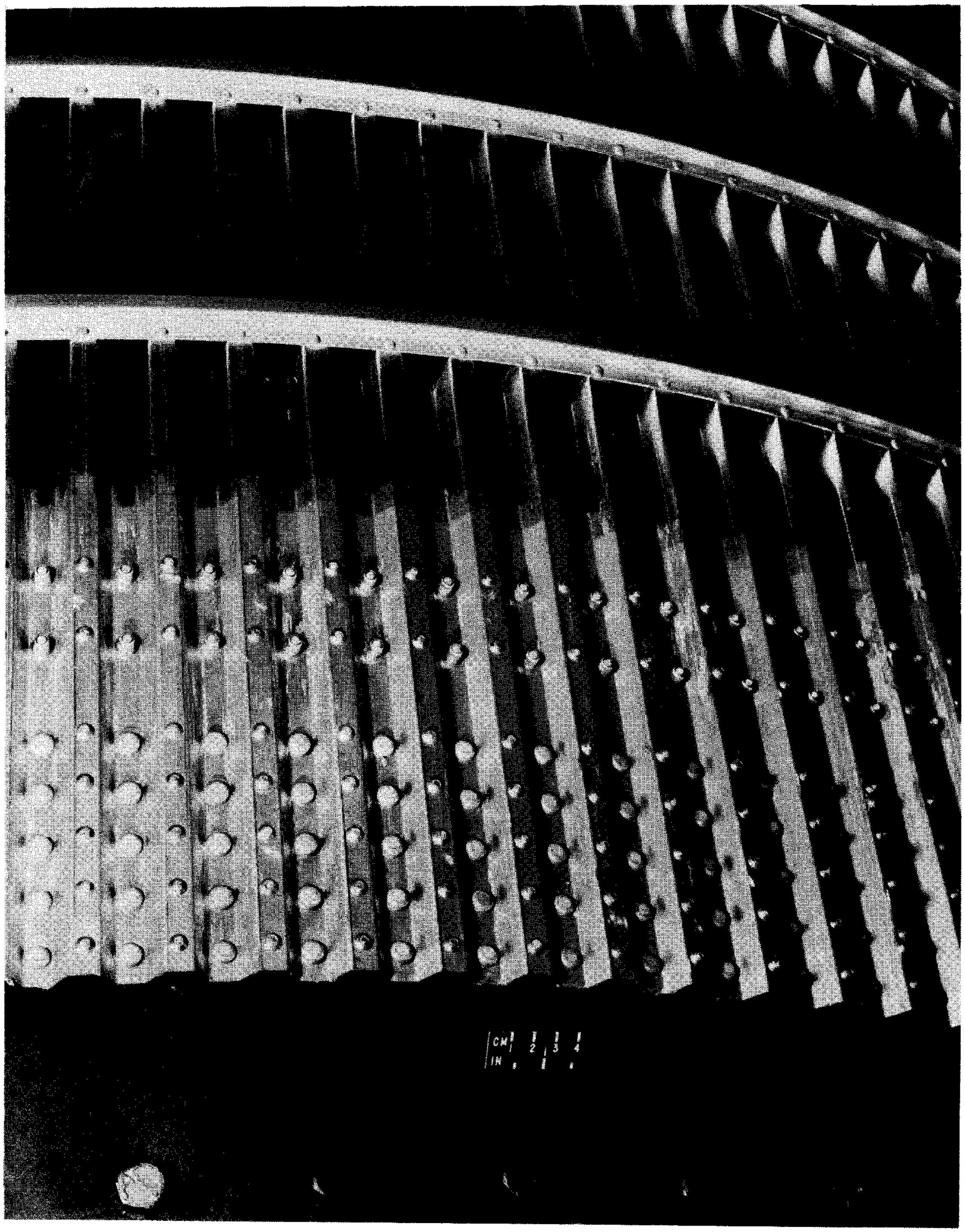


(b) Stiffening ring attachment. L-65-6872

Figure 1.- Concluded.

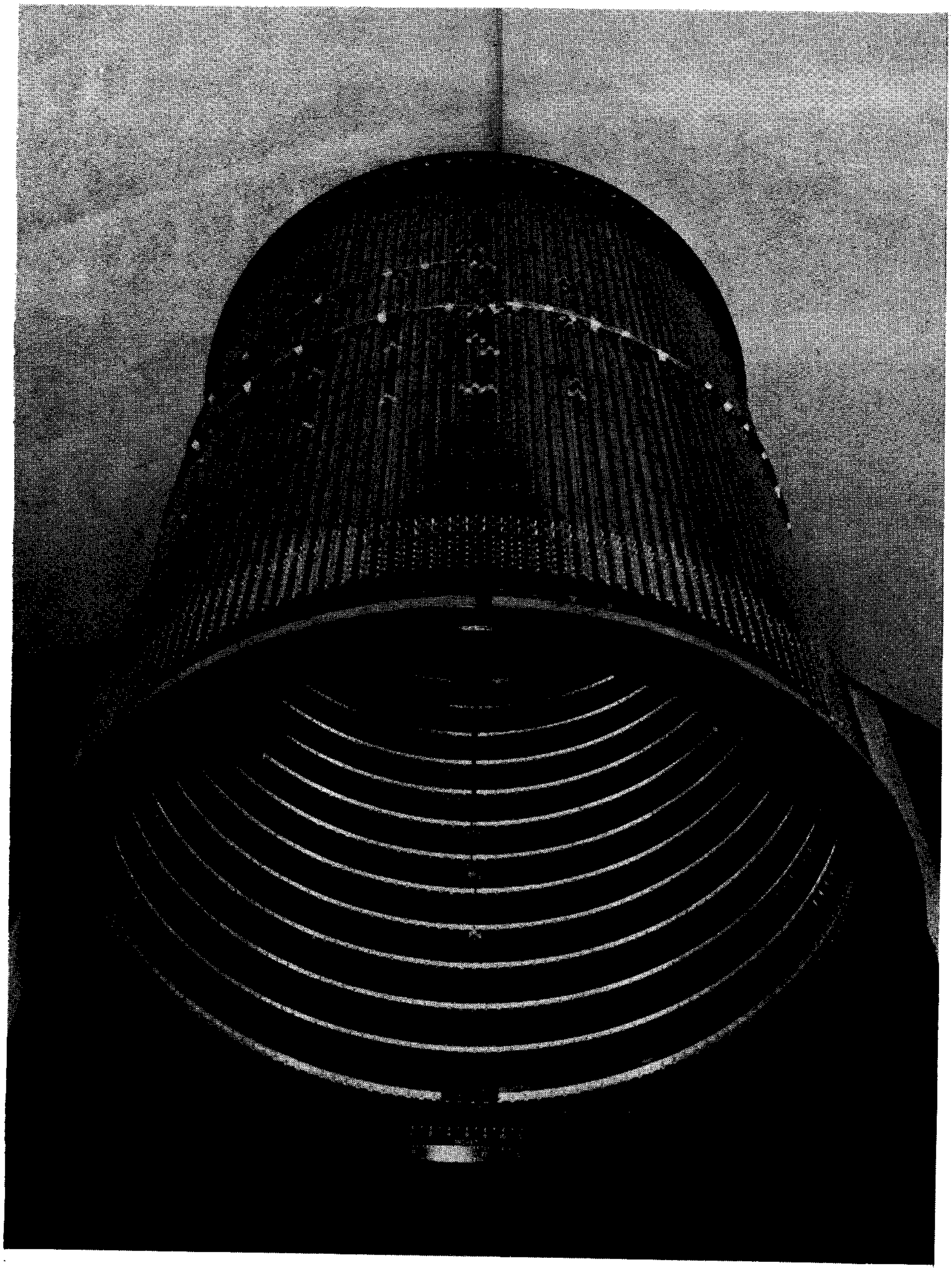

(a) General view.

L-65-6892

Figure 2.- Cylinder 2. Internally stiffened corrugated cylinder.


(b) Stiffening ring attachment. L-65-6893

Figure 2.- Concluded.

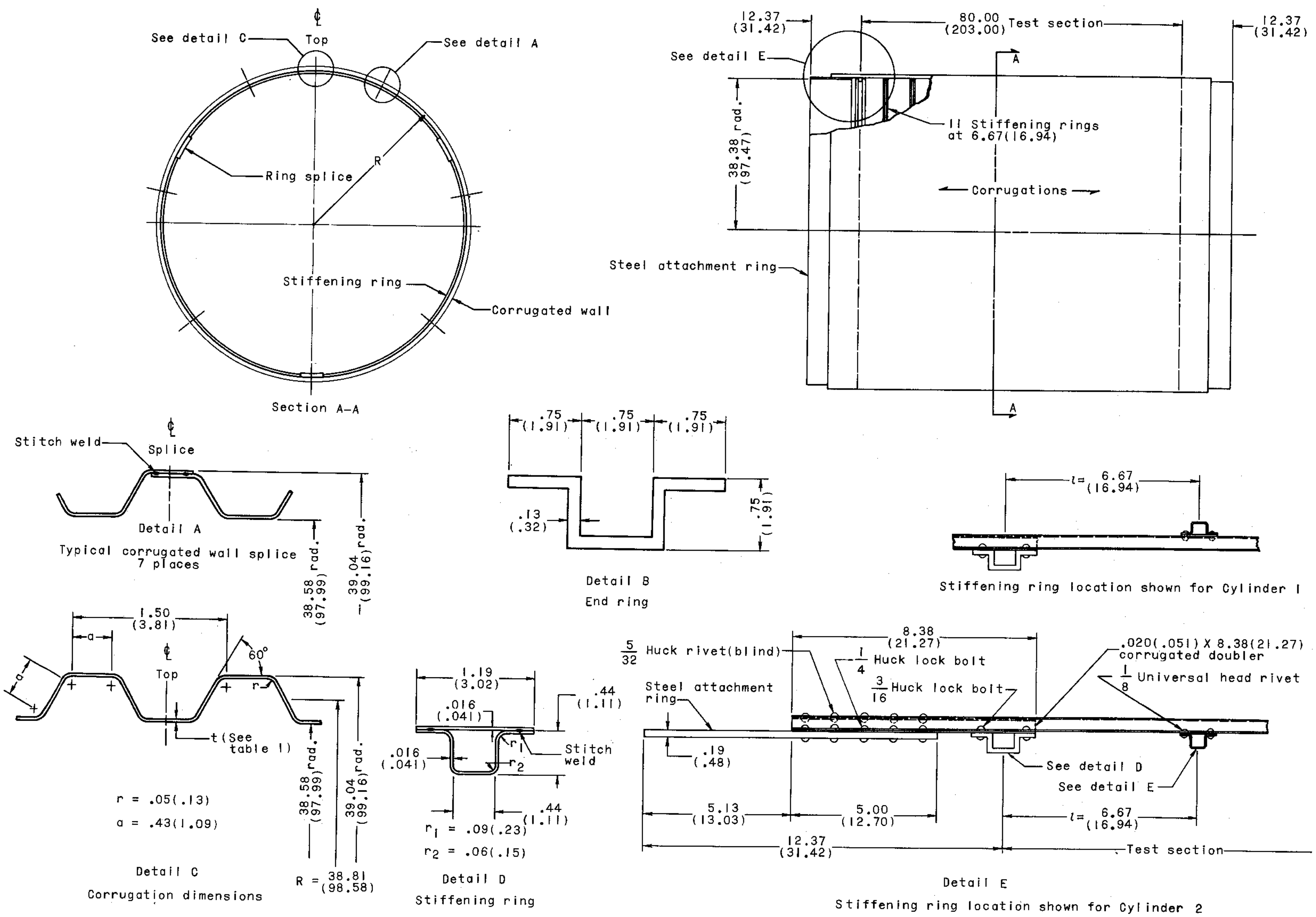


Figure 3.- Construction details of test cylinders. (All dimensions are in inches with centimeter equivalents in parentheses.)

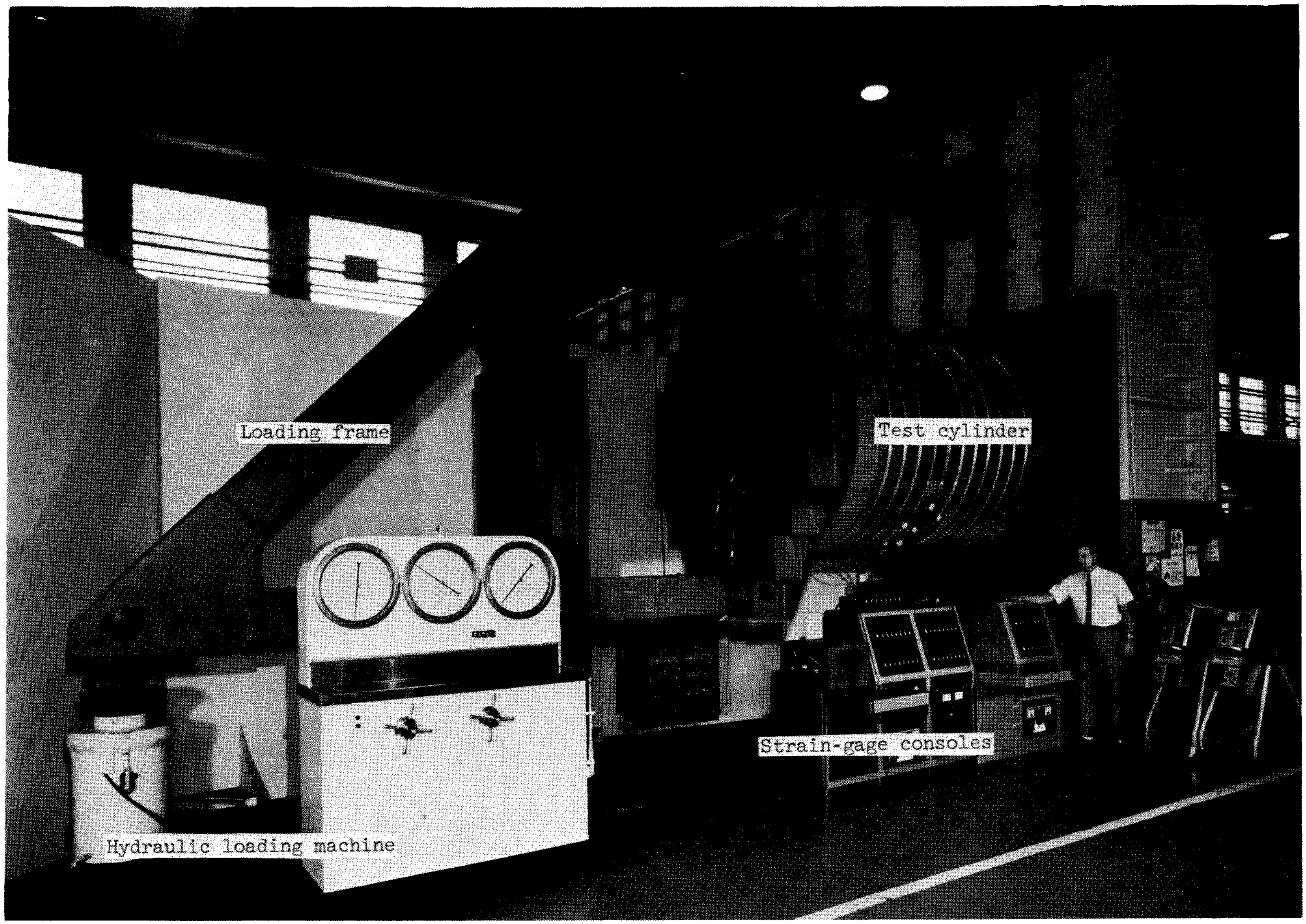


Figure 4.- General view of test facility. L-65-6873

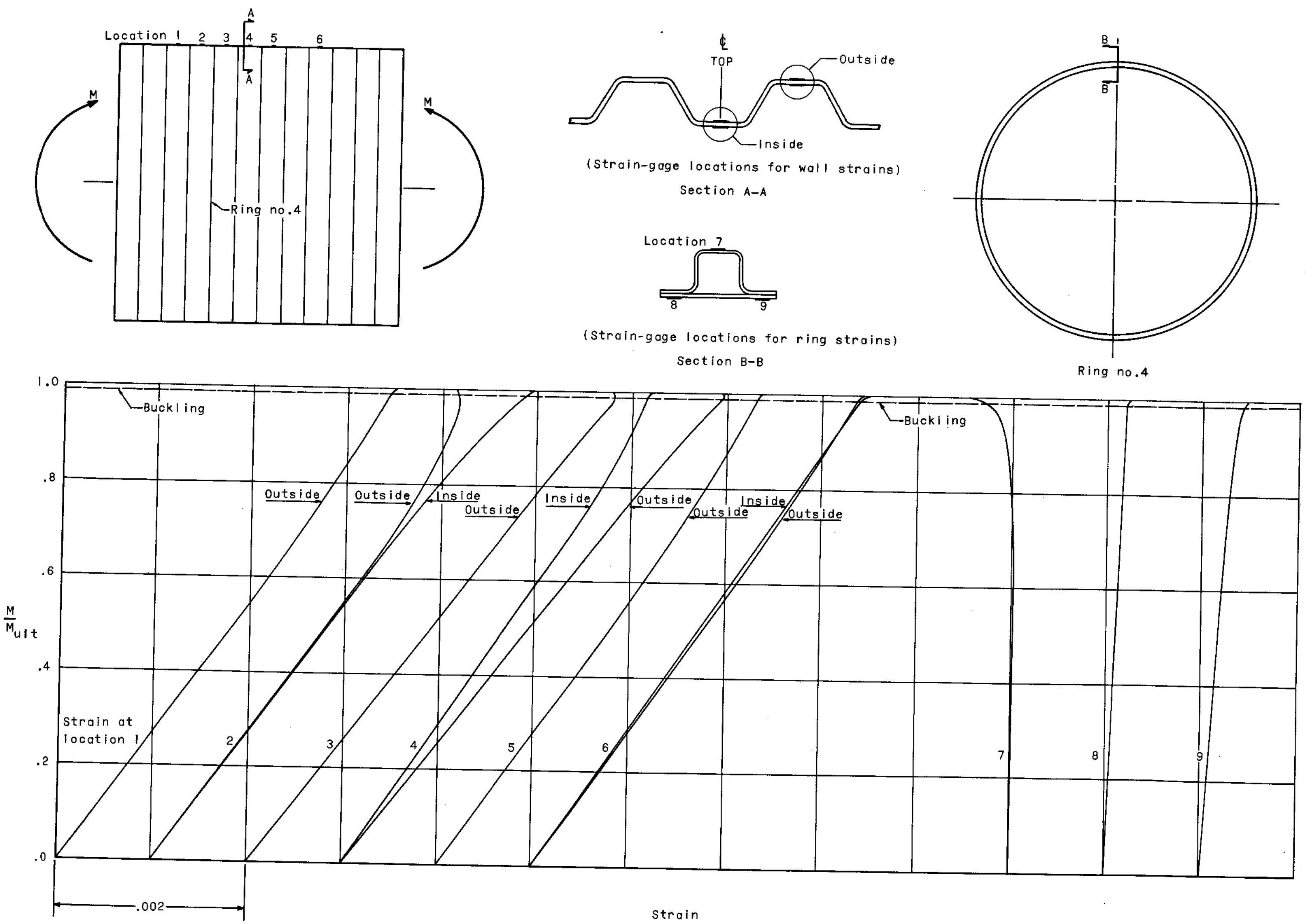


Figure 5.- Measured strains in cylinder 1.

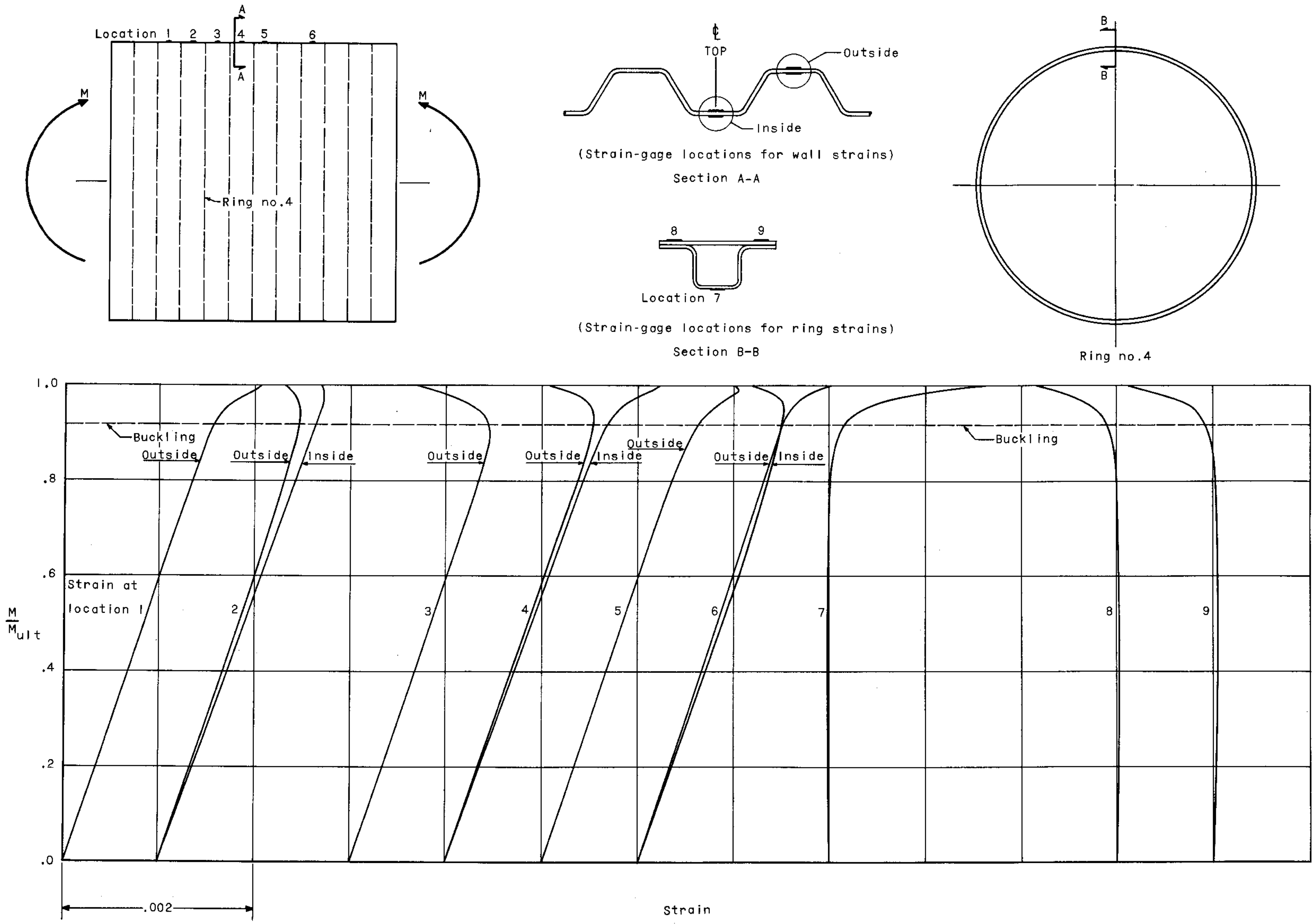


Figure 6.- Measured strains in cylinder 2.

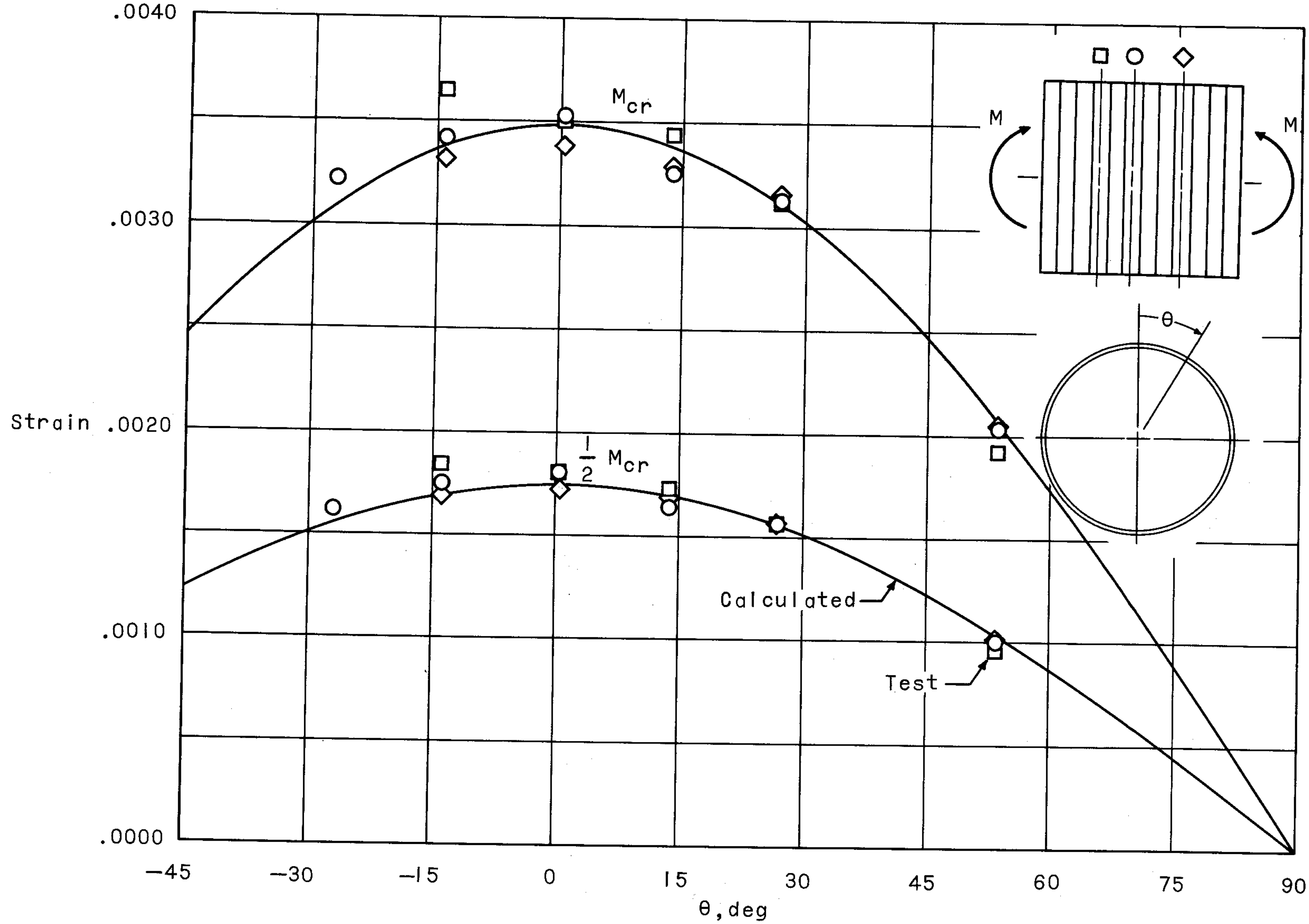


Figure 7.- Comparison between measured and calculated strain distribution for cylinder 1.

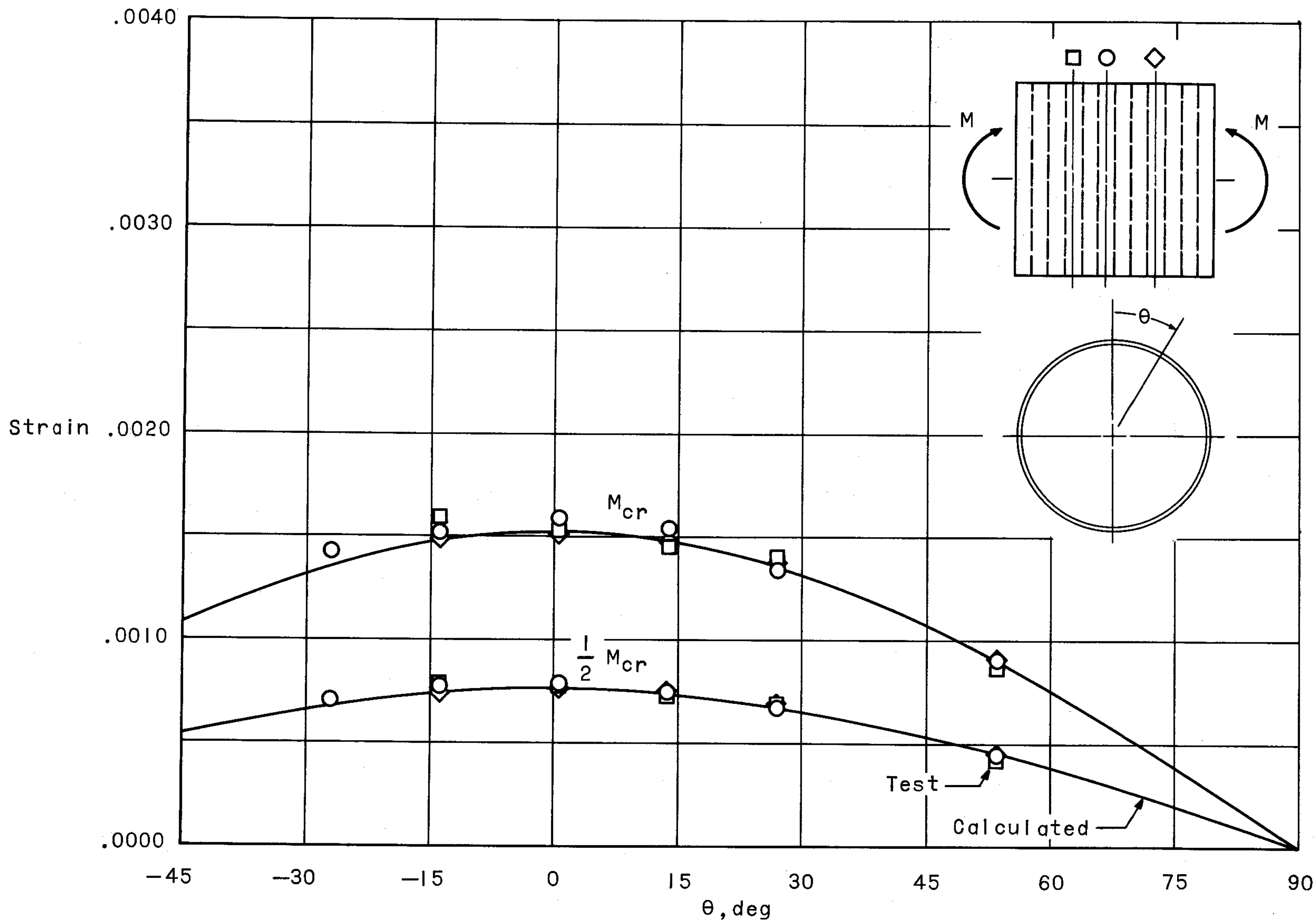


Figure 8.- Comparison between measured and calculated strain distribution for cylinder 2.

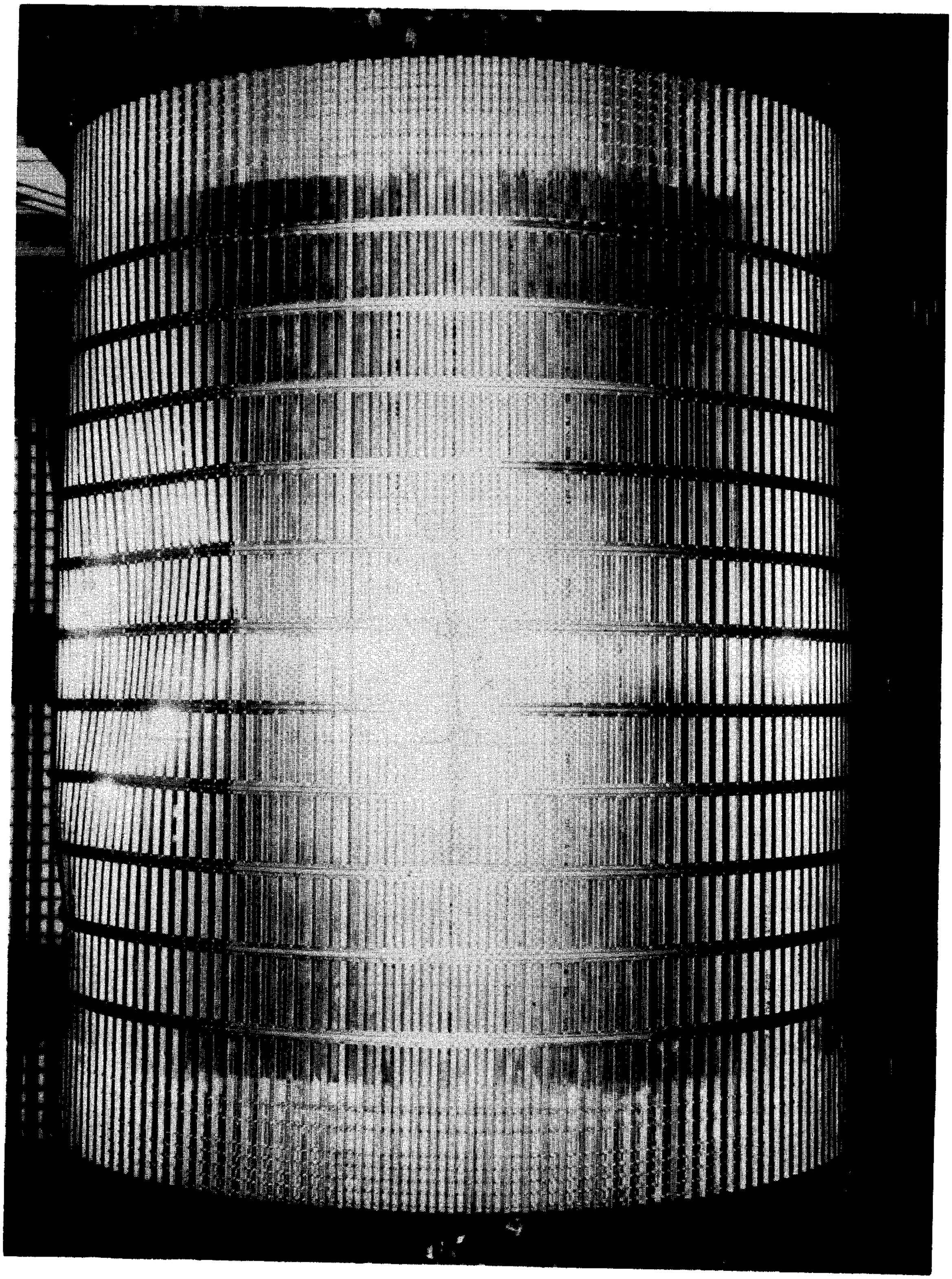

L-65-6867

Figure 9.- Side view of cylinder 1 at failure.

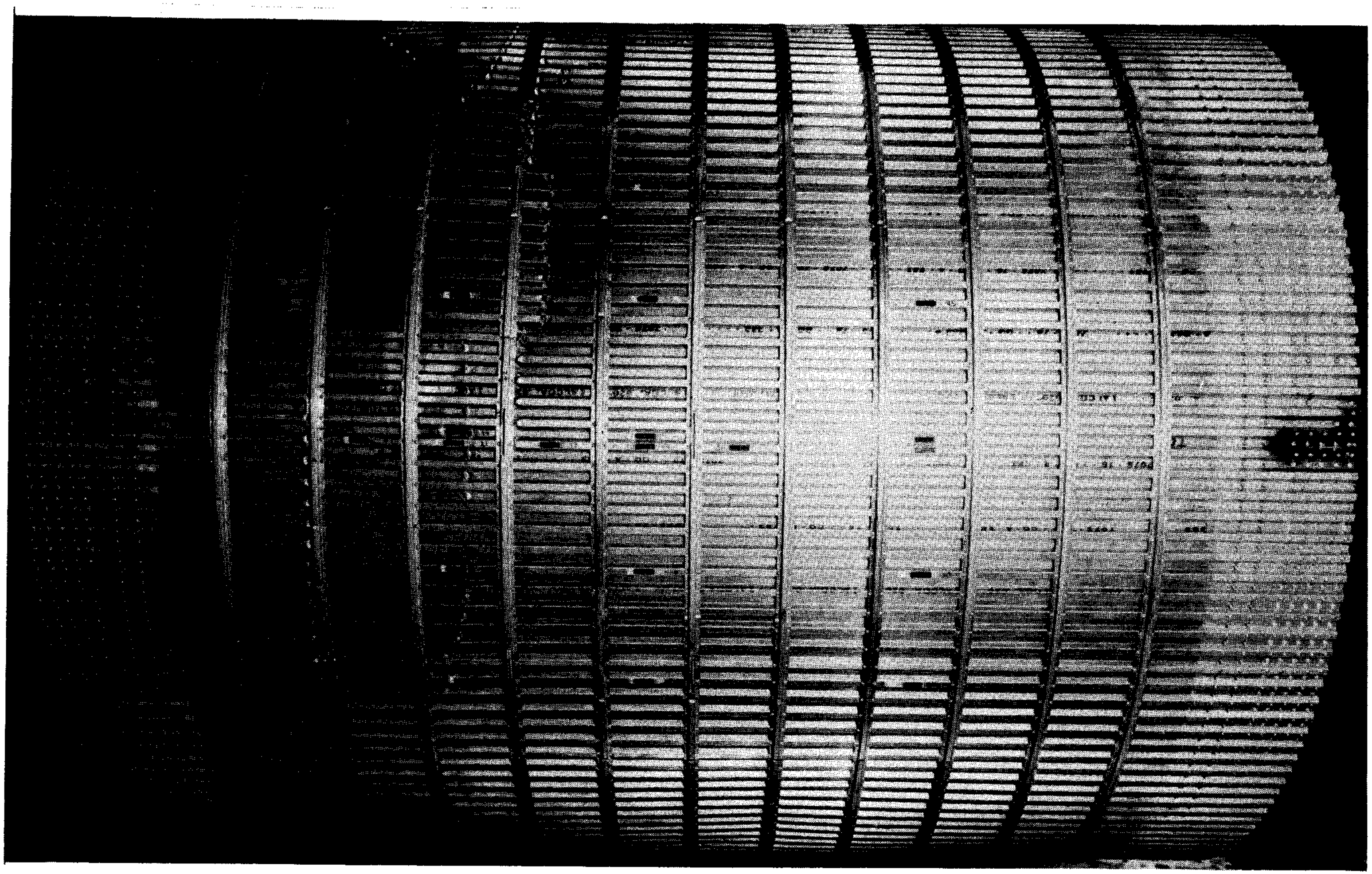

Figure 10.- Top view of cylinder 1 after unloading.

L-65-6874

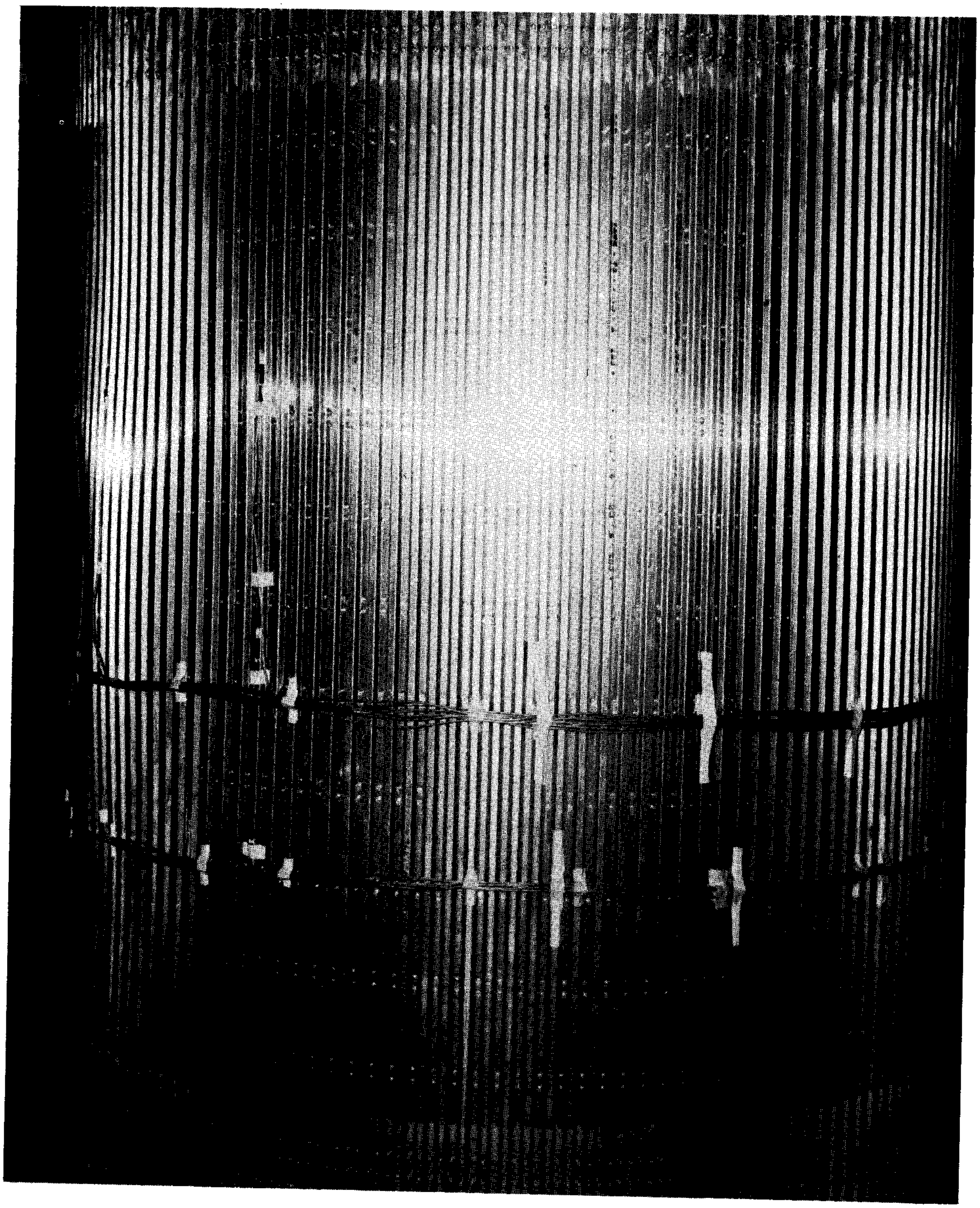

L-65-7171

Figure 11.- Side view of cylinder 2 at failure.

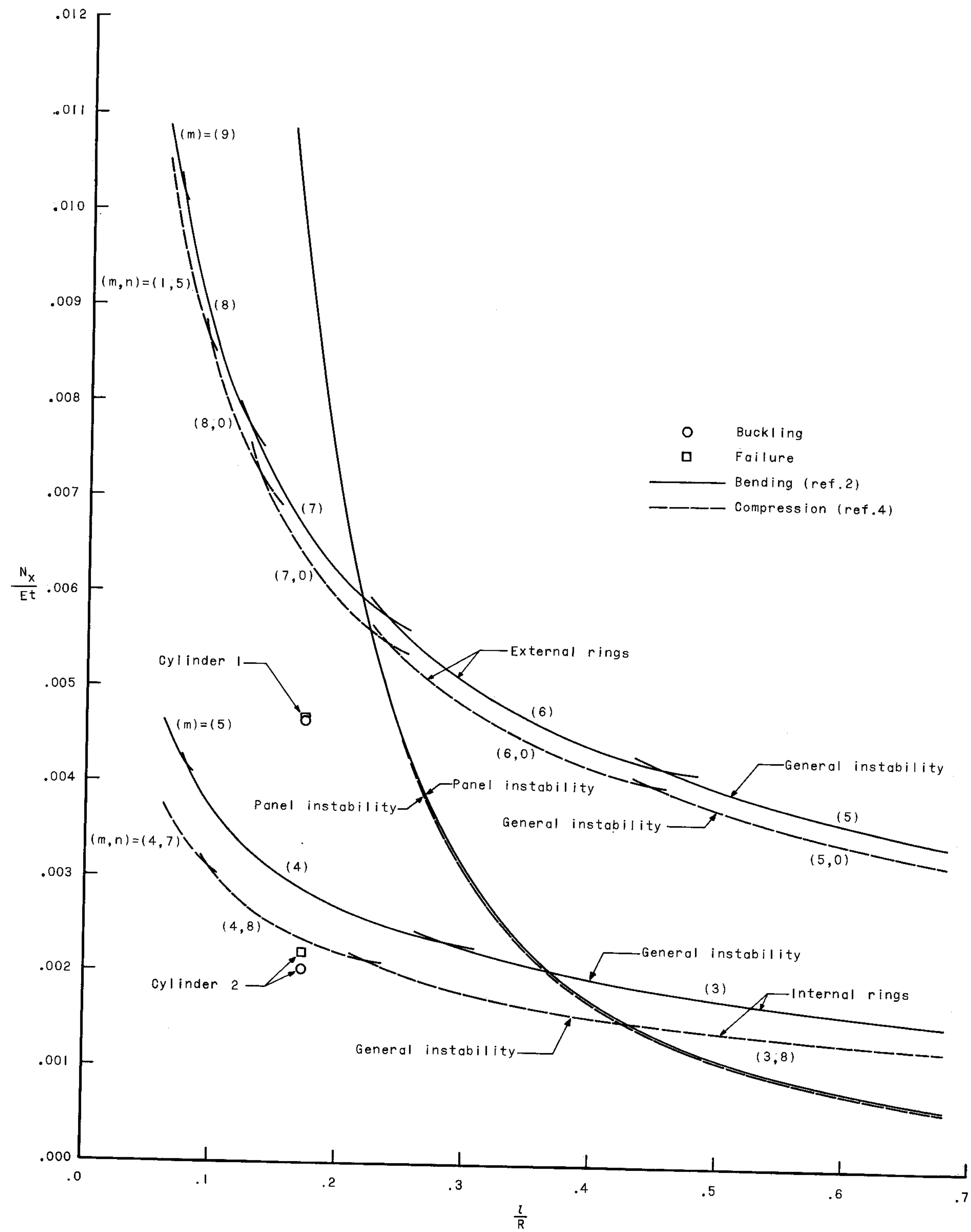


Figure 12.- Comparison between test results and theoretical predictions.